photonics

MDPI

Article

Nd:YVO_4 Random Laser with Preferential Emission at 1340 nm over 1064 nm

Jessica Dipold [1], Luciana R. P. Kassab [2] and Niklaus U. Wetter [1,*]

[1] Instituto de Pesquisas Energéticas e Nucleares, Comissão Nacional de Energia Nuclear—IPEN, São Paulo 05508-000, SP, Brazil; jessica.dipold@gmail.com
[2] Faculdade de Tecnologia de São Paulo, CEETEPS, São Paulo 01101-010, SP, Brazil; kassablm@fatecsp.br
* Correspondence: nuwetter@ipen.br

Abstract: Neodymium-doped yttrium vanadate random lasers have presented exceptional efficiency and output power at the 1064 nm emission wavelength. However, emission at 1340 nm has not yet been observed for these random lasers, even though regular bulk lasers have presented many impressive properties in this infrared region. Here, we present a dual-emission Nd^{3+}:YVO_4 pellet random laser, which emits at both 1064 nm and 1340 nm using a 585 nm pump wavelength, showing a new property corresponding to a much lower laser threshold at 1340 nm than with 1064 nm.

Keywords: random laser; crystal powder; neodymium-doped material

Citation: Dipold, J.; Kassab, L.R.P.; Wetter, N.U. Nd:YVO_4 Random Laser with Preferential Emission at 1340 nm over 1064 nm. *Photonics* **2024**, *11*, 898. https://doi.org/10.3390/photonics11100898

Received: 13 August 2024
Revised: 10 September 2024
Accepted: 23 September 2024
Published: 25 September 2024

1. Introduction

Since being proposed by Letokhov et al. [1] in the 1960s, random lasers (RLs) have been studied for several materials, showing different properties and applications, such as microfluidics [2], speckle-free optical imaging [3] or sensors [4]. Random lasers are not only more cost-effective and easier to fabricate than bulk lasers, but they are also more versatile in terms of material selection. These materials can be colloidal suspensions [5], aerogels [6], dyes [7], crystal powders [8] and glasses [9]. Doped crystals have been frequently used as random laser sources. In particular, neodymium (Nd^{3+})-doped crystals have presented high-quality results for random lasing [8,10,11], with studies focused on their main infrared emission at 1064 nm ($^4I_{11/2} \rightarrow {}^4I_{9/2}$) while pumped at 806 nm ($^4I_{9/2} \rightarrow {}^4F_{5/2}$). Nd^{3+} usually presents two other emission bands in the near-infrared region, one at 1340 nm ($^4I_{13/2} \rightarrow {}^4I_{9/2}$) and another at 1540 nm ($^4I_{15/2} \rightarrow {}^4I_{9/2}$). The 1064 nm emission has a much higher cross-section than both of these emissions. They are less frequently studied due to difficulties of observation, since suppression of the 1064 nm band is necessary to improve emission for these other wavelengths. There are studies of 1340 nm emission for regular bulk lasers made of Nd^{3+}-doped crystals, which have presented good results for pumping at 806 nm [12] or 880 nm ($^4I_{9/2} \rightarrow {}^4F_{3/2}$) [13]. There has also been work on fiber random lasers, which work on the principle of weak Rayleigh scattering and Raman amplification in long fibers, which have shown random laser emission at 1340 nm [14]. To the best of our knowledge, apart from the aforementioned studies, the only other work that has observed emission in a random laser at 1340 nm using a 585 nm pump was conducted by our research group [9].

In the previous work [9], we observed 1340 nm emission of an Nd^{3+}-doped tellurite glass powder random laser pumped at 585 nm ($^4I_{9/2} \rightarrow {}^4G_{5/2}$ & $^2G_{7/2}$), which is another strong absorption band of neodymium. This particular wavelength is rarely employed as a pump source for Nd^{3+}-doped bulk or random lasers [9,15]. Heavy metal oxide glasses have proven to be highly useful for numerous photonic devices, such as waveguides and amplifiers [16,17]. Given the promising results obtained with this pump configuration [9,15], we extended our investigation to other materials, specifically focusing on crystals, which are generally more efficient than glasses, to assess the feasibility of achieving 1340 nm

emission under the same experimental setup. We present a study of a yttrium vanadate crystal doped with neodymium (Nd^{3+}:YVO_4), which was previously examined as a random laser by our research group [8], yielding exceptional results for 1064 nm emission when pumped at 806 nm using a diode laser. In that research, a slope efficiency of 50% as a function of absorbed pump power was found using a regular diode as a pump, which is one of the highest efficiencies achieved for a random laser [18]. In the current research, the excitation was performed with an OPO laser at 585 nm using nanosecond laser pulses, and the emission was observed in both the spectral and time domains. Laser emission was observed at 1064 nm and 1340 nm, with distinct lasing thresholds. Notably, contrary to expectations, the lasing threshold for the 1340 nm emission was approximately three times lower than that for the 1064 nm emission—a phenomenon observed for the first time, to our knowledge, in Nd^{3+}-doped crystals.

2. Materials and Methods

The studied samples were prepared with a Nd^{3+}:YVO_4 crystal with 1.33 mol% neodymium doping, which has a refractive index of 2.04 [8]. The crystal was crushed into a powder and sieved to separate it into different sizes, then washed with isopropyl alcohol to obtain a monodispersed distribution [8]. The powders were pressed and turned into pellets with 5 mm diameter and ~1 mm height, with four different particle-size ranges: 20 to 45 µm (B2), 45 to 75 µm (B3), 75 to 106 µm (B4) and 106 to 150 µm (B5). The samples were further characterized in a previous work by our group [8].

Based on our latest work of a glass random laser [9], the sample was excited with a 585 nm pulsed laser beam, with a pulse duration of 10 ns and a repetition rate of 20 Hz, using an OPOTek model OPOlette. This wavelength was chosen due to its high absorption, as shown in Figure 1a, whose measurement was performed with a Cary 5000 spectrometer (Agilent, Santa Clara, CA, USA). We also measured emission for excitation for 806 nm to observe the differences compared to 585 nm, as shown in Figure 1b. It is possible to notice that 1064 nm has a higher emission for 806 nm excitation than for 585 nm, showing a possible suppression of this band when pumped at 585 nm.

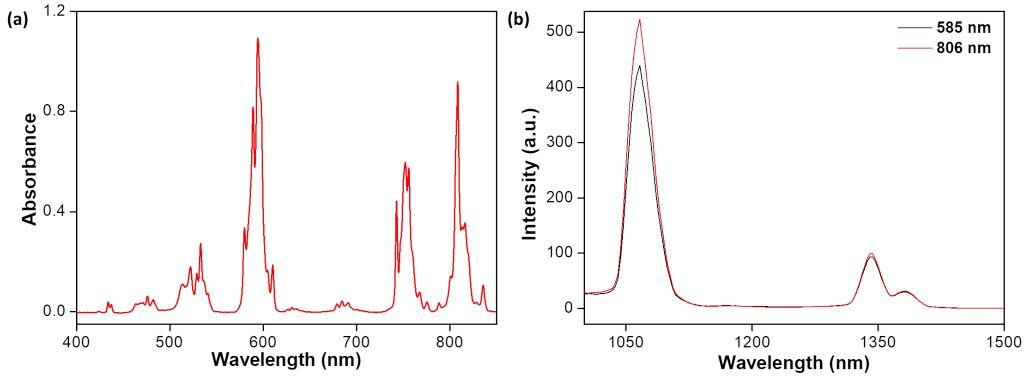

Figure 1. (**a**) Absorption spectrum of the Nd^{3+}:YVO_4 with 1.33 mol% used. (**b**) Emission spectra for 585 nm and 806 nm pump wavelengths normalized by the 1340 nm emission using the exact same pumping and measurement setup.

Laser emission measurements were taken for 1064 nm and 1340 nm. For 1064 nm, two different analyses were made, one using a spectrometer (OceanOptics HR2000, OceanOptics®, Orlando, FL, USA, with 0.24 nm resolution), obtaining the linewidth narrowing and emission intensity, and another using an InGaAs photodetector (Thorlabs DET01CFC, 1.2 GHz, Thorlabs Inc., Newton, NJ, USA), obtaining the rise time and emission intensity through temporal measurements [19]. For 1340 nm, only temporal measurements were made, since the only spectrometer available in our lab for this wavelength range (OceanOptics NIRQUEST, OceanOptics®, Orlando, FL, USA) has a lower resolution than needed for

linewidth narrowing studies, with a resolution limit of 2.7 nm when using a 50 µm diameter fiber.

The experimental setup is shown in Figure 2. In order to separate the 1064 nm and 1340 nm emissions, different filter setups had to be used in front of the photodetector. For both emissions, longpass filters of 700 nm and 1000 nm were added. To isolate the 1340 nm emission, a 1250 nm longpass filter was utilized. The efficacy of this filter was confirmed by setting the OPO to emit at 1064 nm and verifying that no signal was detected by the photodetector, even at the most sensitive voltage range. For the 1064 nm measurements, two mirrors with 98% reflectance for wavelengths higher than 1100 nm were employed to eliminate the 1340 nm emission, which was also generated during testing with the OPO. This precaution was necessary due to the high sensitivity of the photodetector, which has a maximum peak power of 18 mW and is capable of detecting very low emission intensities, particularly in the 1300 nm range.

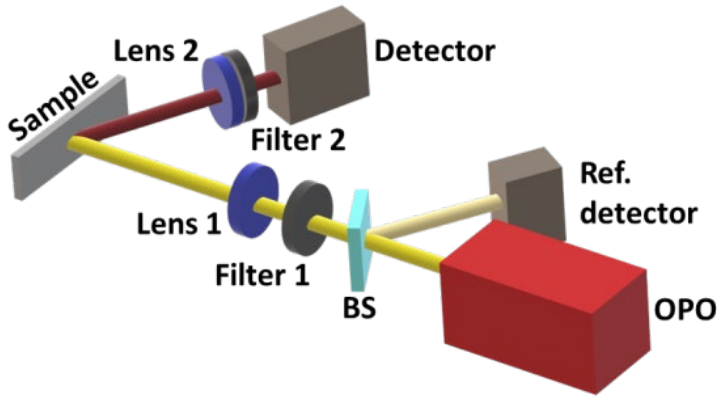

Figure 2. Experimental setup for laser emission measurements. BS: beam splitter, reflecting ~3.2% of the pump beam to a reference detector; Filter 1: shortpass filter of 600 nm; Lens 1: 15 cm focal length lens, focusing the pump beam on the sample surface; Lens 2: telescope with 25 mm and 30 mm focal length lenses to obtain the smallest focus possible; Filter 2: 700 nm and 1000 nm longpass filters combined with either a 1250 nm filter or two highly reflective mirrors for wavelengths of 1100 nm and higher; detector is either an optical fiber (200 µm) connected to a spectrometer or an InGaAs fast photodetector, depending on the type of measurement.

To obtain the spectra, an HR2000 OceanOptics® spectrometer with the SpectraSuite® program was used. To obtain the measurement without damaging the sample, a single pulse was shot, with the integration time being 1 s. This long integration was used to allow a single operator enough time between pressing the single-pulse button and taking the measurement itself. The sample was then repositioned using a micrometer, ensuring the next pulse would not fall on the same spot. For temporal measurements, a single-pulse emission was taken using the single-shot option in the oscilloscope, and an average of four pulses was made, shifting the sample between them.

In the measurements taken with the spectrometer, the emission peak at 1064 nm was fitted and its maximum value and full-width half maximum (FWHM) were obtained. Examples of the emitted peaks for low and high pump energies at this wavelength are shown in Figure 3a for sample B4. Even though it was not possible to perform the FWHM analysis for 1340 nm, we observed its emission through the spectrometer as well, with results shown in Figure 3b. For the temporal measurements, two different procedures were performed using the emission observed with an oscilloscope. The first one used a Python code developed by the author to find the rise time, which is the difference between the time from the beginning of the emission to its maximum. When laser occurs, a small peak of ~5 ns width appears, and the rise time reaches its smallest value. To obtain the emission intensity, only energies where the short peak of the laser emission was larger than the spontaneous emission peak, which has a longer duration, were considered. A signal with only spontaneous emission was subtracted from

signals with laser emission in order to obtain the intensity of stimulated emission, which was used to find the laser threshold. Examples of studied data are shown in Figure 3c.

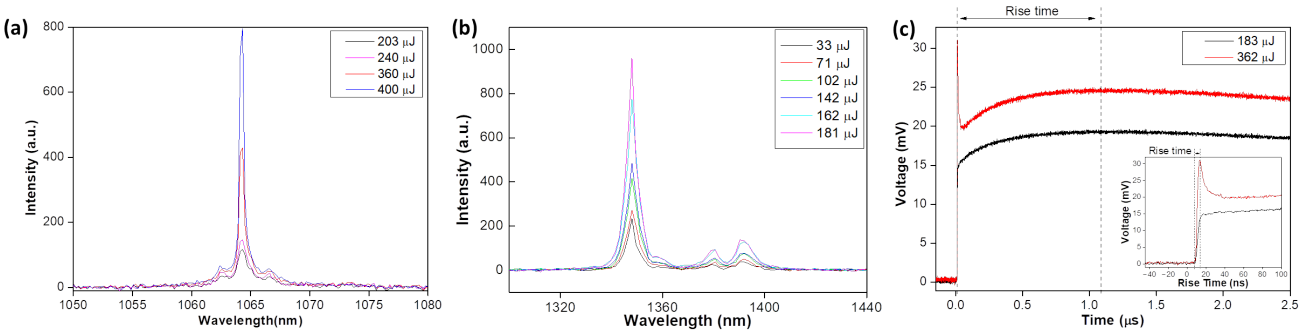

Figure 3. For sample B4, examples of (**a**) spectrometer measurements for different pump energies for emission at 1064 nm; (**b**) spectrometer measurements for different pump energies for emission at 1340 nm; and (**c**) temporal measurements for different pump energies for emission at 1064 nm, showing how the rise time is measured for low energy, with inset showing a zoom of the ~5 ns peak which appears after laser threshold, and its rise time.

3. Results

3.1. 1064 nm Measurements

For the emission at 1064 nm, it was possible to obtain results through two different methods: spectral and temporal.

Using the spectrometer, the linewidth narrowing was measured by calculating the full-width half maximum (FWHM) of the emission peak at 1064 nm, which is shown in Figure 3a. All pellets presented an initial FWHM of ~1.2 nm, narrowing to ~0.4 nm after a certain threshold (Figure 4a). The fitting is of a Boltzmann curve (sigmoidal) and is used to find the inflection point, which is considered the threshold. It is clear that the lowest threshold is presented for sample B4 (292 μJ), while the longest is for samples B2 and B5 (330 μJ). In Figure 4b, the peak value for the 1064 nm emission obtained by the spectrometer was plotted, presenting a clear laser behavior, with two lines of different slopes meeting at a threshold point. The first slope is not zero due to the large size of the optical fiber used (200 μm), which collected light emitted from both stimulated and spontaneous emission. The threshold values are in agreement with the ones found for the FWHM measurements. Both can be viewed and compared in Table 1.

Figure 4c shows the rise time obtained for the studied samples, showing a decrease from ~2 μs to ~6 ns. For this measurement, the laser threshold corresponds to the pump energy where the lowest rise time value is found [19]. The lowest threshold in this case is observed for B2, followed by B3, B4 and B5; that is, the smaller the particles, the lower the threshold.

Table 1. Threshold values for spectrometer measurements (FWHM and intensity) and oscilloscope measurements (rise time and intensity) for all samples emitting at 1064 nm.

	Spectrometer		Oscilloscope	
Sample	**Threshold from FWHM (μJ)**	**Threshold from Intensity (±10 μJ)**	**Threshold from Rise Time (μJ)**	**Threshold from Intensity (±10 μJ)**
B2	327 ± 3	300	240 ± 10	220
B3	315 ± 2	293	260 ± 10	240
B4	292 ± 2	290	310 ± 20	280
B5	330 ± 1	310	320 ± 20	310

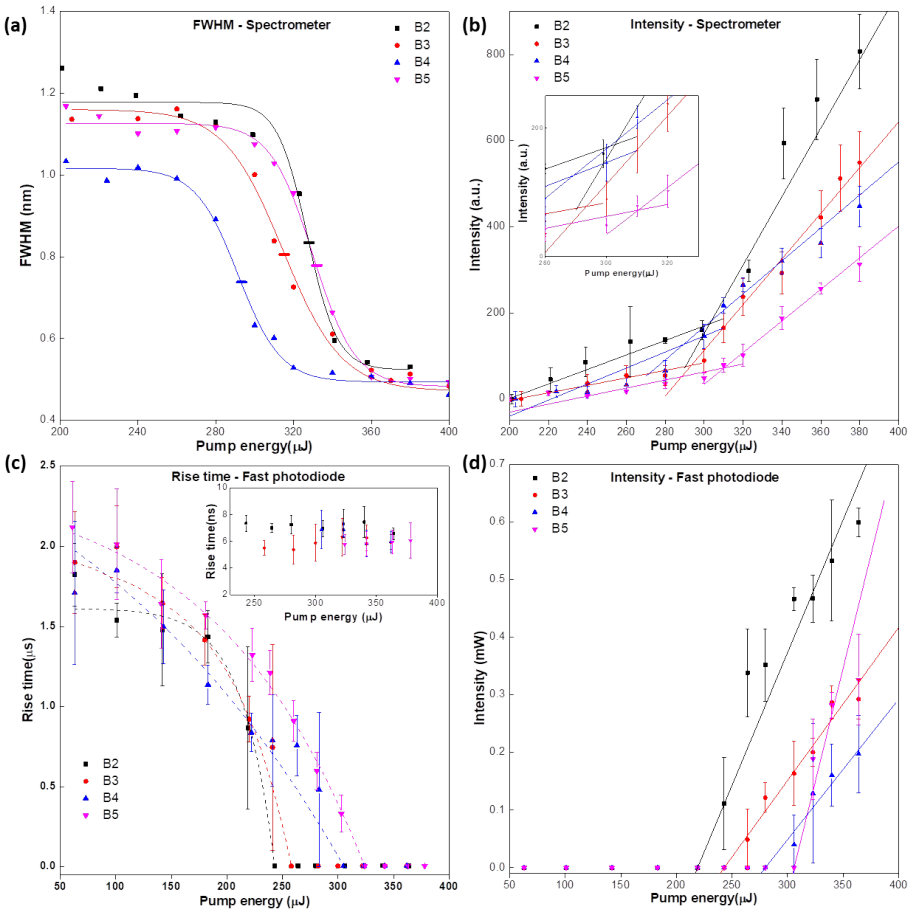

Figure 4. Measurements for 1064 nm emission in B2 (black squares), B3 (red circles), B4 (blue triangles) and B5 (magenta inverted triangles): (**a**) FWHM variation measured with a spectrometer; (**b**) intensity variation measured with a spectrometer, with the inset showing a zoom in the threshold region; (**c**) rise time decay, measured with a photodetector, with inset showing a zoom of the constant rise time region after 240 μJ; and (**d**) intensity variation measured with a photodetector. Error bars are standard deviations of the measurements taken for each point.

Following the procedure outlined in the Methods section, we subtracted the spontaneous emission from the plots containing the short laser pulse, resulting in the intensities presented in Figure 4d. The data confirmed a consistent trend in rise time, with increasing values correlating with particle size. The initial slope is zero, as spontaneous emission had been entirely excluded from consideration. Notably, the B5 curve displayed a steeper slope compared to the other curves, which is likely attributable to increased measurement error.

3.2. 1340 nm Measurements

To observe emission at 1340 nm, temporal measurements were made, and the results are shown in Figure 5.

The rise time variation for sample B5 is from 3 μs to 10 ns; for B4, it is from 2.4 μs to 6 ns; for B3, it is from 1.7 μs to 5.4 ns; and for B2, it is from 1.5 μs to 5 ns. On average, after lasing all samples had about 0.33% of the initial rise time. According to Shi et al. [19], the laser threshold is the first point where the rise time stabilizes, i.e., when it reaches its lowest value. The thresholds obtained through this method are shown in Table 2. We can see that the lowest threshold is found for sample B2, followed by B3, B4 and B5. This follows the result verified for 1064 nm, demonstrating that for this pump wavelength, smaller particles present the lowest thresholds.

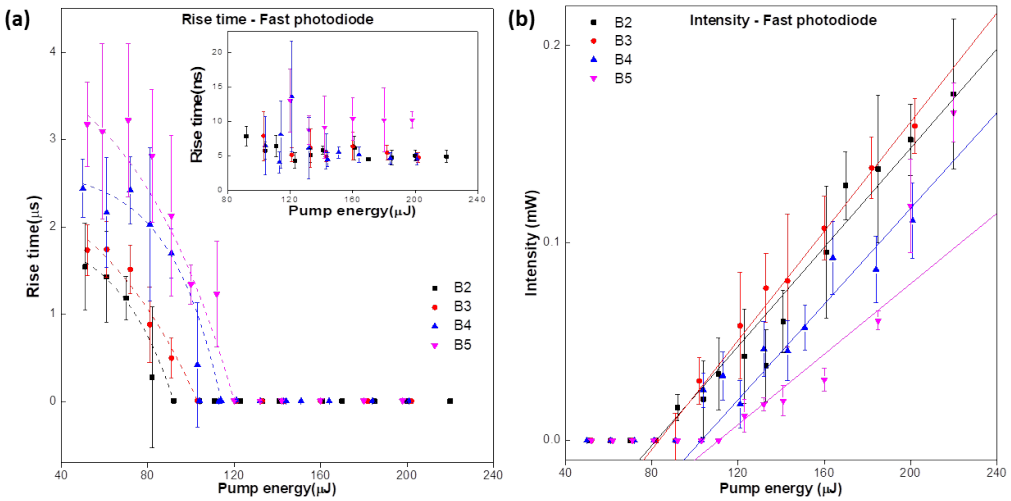

Figure 5. For 1340 nm emission: (**a**) rise time measurements, with the inset showing a zoom of the shortest rise time after 80 μJ pump energy; (**b**) intensity measured with the photodetector. Error bars are standard deviations of the measurements taken for each point.

Table 2. Summary of threshold energies for 1340 nm emission.

Sample	Oscilloscope	
	Threshold from Rise Time (±10 μJ)	**Threshold from Intensity (±10 μJ)**
B2	90	80
B3	100	90
B4	110	100
B5	120	110

The intensity results corroborate this theory, showing the same thresholds as those seen through the rise time within errors.

It is clear that the sample starts lasing at 1340 nm earlier than at 1064 nm, at approximately one-third of the pump energy.

For 1064 nm measurements, the observed thresholds across all samples were consistently in the 300 μJ range, as measured by both the spectrometer and oscilloscope. This emission behavior is in agreement with our previous study of bulk Nd^{3+}:YVO_4 [8], with optimal results for intermediate particle sizes B3 and B4. For 1340 nm measurements, the threshold increased with particle size, with sample B2 displaying the lowest value and sample B5 the highest value. The remaining samples displayed similar threshold values. This trend, where smaller particles exhibit lower thresholds and higher emission intensities, mirrors findings in our previous research using the Nd^{3+}-doped glass random laser [9], where laser emission was not observed for particles larger than 20 μm, with successful operation only observed for particles around 5 μm, and with emission at 1340 nm only.

Therefore, for both emissions, the threshold was shortest for sample B2, which is made from the smallest-sized particles (between 20 and 45 μm). Comparing both, we can see that the threshold for 1064 nm is more than two times higher at 1340 nm for every sample (220 μJ and 80 μJ for B2, 240 μJ and 90 μJ for B3, 280 μJ and 100 μJ for B4 and 310 μJ and 110 μJ for B5). These findings are corroborated by the fact that the values measured for 1064 nm through traditional linewidth narrowing measurements were even higher. To the best of our knowledge, this is a previously unreported phenomenon.

4. Discussion

Given that both the 1064 nm and 1340 nm emissions originate from the same upper laser level ($^4F_{3/2}$), the difference in thresholds cannot be attributed to mechanisms such as excited-state absorption or up-conversion, as these processes would influence both emissions similarly. The difference is also not due to increased scattering at the 585 nm wavelength compared to the 806 nm wavelength, as the scattering length in this regime is approximately equal to the particle sizes [20]; that is, the pumping density does not change between the two different pump wavelengths in our specific particle-size regime. Moreover, the difference in thresholds is not due to variations in the penetration length or the critical volume within the laser pellets. This is evidenced by the absorption spectrum shown in Figure 1a, which indicates that the absorption lengths for 585 nm and 806 nm are similar. Considering the residence time (τ_{res}) of the pump within the powder, as calculated from ref. [20], it is approximately 18% greater for 585 nm pumping than for 806 nm, due to the slightly larger absorption length of the shorter pump wavelength. This is still not enough to explain the threshold difference.

It is important to observe that the emission at 1064 nm is still more efficient than at 1340 nm, with intensities reaching ~0.6 mW for B2 at 1064 nm, while at 1340 nm, the maximum emission intensity is 0.4 mW (both measurements taken at 364 µJ of the pump). The higher threshold and higher slope efficiency at 1064 nm are similar to that which is observed from reabsorption in, for example, ytterbium oscillators [21]. In reference [9], we suggested that heating of the lower laser level of the 1064 nm transition at the 20 Hz repetition rate might be a motive for this reabsorption and calculated an approximate sample temperature of 835 degrees Celsius of the TZA glass. This heating is larger for 585 nm than for 806 nm pumping, since the quantum defect is much higher for the lower wavelength.

We believe that the following order of effects might be occurring in our system: After absorption of a pump photon at 585 nm, cross-relaxation between two neighboring neodymium ions transfers them to the $^4I_{13/2}$ energy level ($^4F_{3/2} \rightarrow {}^4I_{13/2}$ & $^4I_{9/2} \rightarrow {}^4I_{13/2}$). Next, an energy transfer up-conversion occurs, bringing ions from $^4I_{13/2}$ to the $^4G_{9/2}$ + $^4G_{11/2}$ + $^2K_{15/2}$ level, depopulating this level and increasing the possibility of laser emission at 1340 nm. This could occur due to the pump laser intensity, which increases the temperature of the system and allows this transition to occur.

5. Conclusions

A random laser is distinguished by the absence of a traditional resonant cavity, with light amplification occurring through multiple scattering events within the gain medium. This intrinsic randomness complicates direct control of the emission wavelength via the pump wavelength. Previous studies have demonstrated wavelength tuning through modifications to the gain medium, adjustments to the scattering medium and the application of external perturbations. In most scenarios, the pump wavelength does not directly influence the laser's output wavelength. The tuning capabilities of techniques such as angle tuning or cavity length adjustment are typically limited, and the substantial wavelength shift from 1064 nm to 1340 nm, achieved by altering the pump wavelength from 800 nm to 585 nm, respectively, is a significant departure from this general trend.

Here, Nd^{3+}:YVO_4 powder pellets random lasers were investigated, showing laser emission for both 1064 nm and 1340 nm using a 585 nm pump wavelength. The threshold for 1340 nm was approximately three times smaller than for 1064 nm, even though it was 34% less efficient. This material should allow for real-time tunability, enabling very fast and precise wavelength switching. Such a material could find many applications in optical communications, where dynamically adjustable laser sources are desired for adaptive modulation formats and wavelength division multiplexing (WDM), and in medical applications, where precision surgery and therapy with wavelength-specific interactions with biological tissues are of interest.

Author Contributions: Conceptualization, N.U.W. and J.D.; methodology, N.U.W. and J.D.; formal analysis, N.U.W. and J.D.; investigation, J.D. and N.U.W.; resources, N.U.W. and L.R.P.K.; data curation, J.D. and N.U.W.; writing—original draft preparation, J.D., N.U.W. and L.R.P.K.; supervision, N.U.W.; project administration, N.U.W.; funding acquisition, N.U.W. and L.R.P.K. All authors have read and agreed to the published version of the manuscript.

Funding: This research was funded by IPEN-CNEN, grant number IPEN/CNEN 2020.06.IPEN.33.PD, São Paulo Research Foundation (FAPESP) (grant no. 2019/06334-4, 2017/10765-5), the National Council for Scientific and Technological Development (CNPq, grant no. 308842/2017-0, 308526/2021-0, 302532/2019-6, 395745/2023-9), the National Institute of Photonics (INCT de Fotônica, 465.763/2014) and Sisfoton (440228/2021-2) projects supported by CNPq.

Data Availability Statement: The data presented in this study are available upon request from the corresponding author.

Acknowledgments: The authors would like to thank Ricardo Samad and Lilia Coronato Courrol for important theoretical discussions, as well as Camila Dias for assisting with some calculations.

Conflicts of Interest: The authors declare no conflicts of interest.

References

1. Letokhov, V.S. Quantum statistics of multi-mode radiation from an ensemble of atoms. *Sov. Phys. JETP* **1968**, *26*, 835–840.
2. Jorge, K.C.; Alvarado, M.A.; Melo, E.G.; Carreno, M.N.P.; Alayo, M.I.; Wetter, N.U. Directional random laser source consisting of a HC-ARROW reservoir connected to channels for spectroscopic analysis in microfluidic devices. *Appl. Opt.* **2016**, *55*, 5393–5398. [CrossRef] [PubMed]
3. Redding, B.; Choma, M.A.; Cao, H. Speckle-free laser imaging using random laser illumination. *Nat. Photonics* **2012**, *6*, 355–359. [CrossRef] [PubMed]
4. Leandro, D.; deMiguel-Soto, V.; López-Amo, M. High-Resolution Sensor System Using a Random Distributed Feedback Fiber Laser. *J. Light. Technol.* **2016**, *34*, 4596–4602. [CrossRef]
5. Jimenez-Villar, E.; da Silva, I.F.; Mestre, V.; Wetter, N.U.; Lopez, C.; de Oliveira, P.C.; Faustino, W.M.; de Sa, G.F. Random Lasing at Localization Transition in a Colloidal Suspension (TiO_2@Silica). *ACS Omega* **2017**, *2*, 2415–2421. [CrossRef] [PubMed]
6. Wetter, N.U.; de Miranda, A.R.; Pecoraro, E.; Ribeiro, S.J.L.; Jimenez-Villar, E. Dynamic random lasing in silica aerogel doped with rhodamine 6G. *RSC Adv.* **2018**, *8*, 29678–29685. [CrossRef] [PubMed]
7. Sha, W.L.; Liu, C.H.; Alfano, R.R. Spectral and temporal measurements of laser action of Rhodamine-640 dye in strongly scattering media. *Opt. Lett.* **1994**, *19*, 1922–1924. [CrossRef] [PubMed]
8. Wetter, N.U.; Giehl, J.M.; Butzbach, F.; Anacleto, D.; Jimenez-Villar, E. Polydispersed Powders (Nd^{3+}:YVO_4) for Ultra Efficient Random Lasers. *Part. Part. Syst. Charact.* **2018**, *35*, 1700335. [CrossRef]
9. Dipold, J.; Bordon, C.D.S.; Magalhaes, E.S.; Kassab, L.R.P.; Jimenez-Villar, E.; Wetter, N.U. 1337 nm Emission of a Nd^{3+}-Doped TZA Glass Random Laser. *Nanomaterials* **2023**, *13*, 1972. [CrossRef] [PubMed]
10. Azkargorta, J.; Iparraguirre, I.; Barredo-Zuriarrain, M.; Garcia-Revilla, S.; Balda, R.; Fernandez, J. Random Laser Action in Nd:YAG Crystal Powder. *Materials* **2016**, *9*, 369. [CrossRef] [PubMed]
11. Moura, A.L.; Maia, L.J.Q.; Jerez, V.; Gomes, A.S.L.; de Araújo, C.B. Random laser in Nd:YBO_3 nanocrystalline powders presenting luminescence concentration quenching. *J. Lumin.* **2019**, *214*, 116543. [CrossRef]
12. Okida, M.; Itoh, M.; Yatagai, T.; Ogilvy, H.; Piper, J.; Omatsu, T. Heat generation in Nd doped vanadate crystals with 1.34 μm laser action. *Opt. Express* **2005**, *13*, 4909–4915. [CrossRef] [PubMed]
13. Pavel, N.; Dascalu, T.; Vasile, N.; Lupei, V. Efficient 1.34-μm laser emission of Nd-doped vanadates under in-band pumping with diode lasers. *Laser Phys. Lett.* **2009**, *6*, 38–43. [CrossRef]
14. Zhang, Y.; Ye, J.; Ma, X.Y.; Xu, J.M.; Song, J.X.; Yao, T.F.; Zhou, P. High power tunable multiwavelength random fiber laser at 1.3 μm waveband. *Opt. Express* **2021**, *29*, 5516–5524. [CrossRef] [PubMed]
15. Camara, J.G.; da Silva, D.M.; Kassab, L.R.P.; de Araujo, C.B.; Gomes, A.S.L. Random laser emission from neodymium doped zinc tellurite glass-powder presenting luminescence concentration quenching. *J. Lumin.* **2021**, *233*, 117936. [CrossRef]
16. da Silva, D.S.; Wetter, N.U.; de Rossi, W.; Kassab, L.R.P.; Samad, R.E. Production and characterization of femtosecond laser-written double line waveguides in heavy metal oxide glasses. *Opt. Mater.* **2018**, *75*, 267–273. [CrossRef]
17. Kassab, L.R.P.; Fukumoto, M.E.; Cacho, V.D.D.; Wetter, N.U.; Morimoto, N.I. Spectroscopic properties of Yb^{3+} doped PbO-Bi_2O_3-Ga_2O_3 glasses for IR laser applications. *Opt. Mater.* **2005**, *27*, 1576–1582. [CrossRef]
18. Gomes, A.S.L.; Moura, A.L.; de Araújo, C.B.; Raposo, E.P. Recent advances and applications of random lasers and random fiber lasers. *Prog. Quantum Electron.* **2021**, *78*, 100343. [CrossRef]
19. Shi, X.Y.; Chang, Q.; Tong, J.H.; Feng, Y.J.; Wang, Z.N.; Liu, D.H. Temporal profiles for measuring threshold of random lasers pumped by ns pulses. *Sci. Rep.* **2017**, *7*, 5325. [CrossRef] [PubMed]

20. Noginov, M.; Zhu, G.; Frantz, A.; Novak, J.; Williams, S.; Fowlkes, I. Dependence of $NdSC_3(BO_3)_4$ random laser parameters on particle size. *J. Opt. Soc. Am. B Opt. Phys.* **2004**, *21*, 191–200. [CrossRef]
21. Matsubara, S.; Ueda, T.; Takamido, T.; Kawato, S.; Kobayashi, T. Nearly quantum-efficiency limited oscillation of Yb:YAG laser at room temperature. In Proceedings of the Conference on Lasers and Electro-Optics (CLEO), Baltimore, MD, USA, 22–27 May 2005.